

# The minor myosin heavy chain, mhcA, of *Caenorhabditis elegans* is necessary for the initiation of thick filament assembly

Robert H. Waterston

Department of Genetics, Washington University School of Medicine,  
660 S. Euclid Avenue, St Louis, MO 63110, USA

Communicated by J.Sulston

*Caenorhabditis elegans* body wall muscle has two distinct myosin heavy chain isoforms, mhcA and mhcB. Mutations eliminating the major isoform, mhcB, have previously been shown to yield paralyzed, viable animals. In this paper we show that the minor isoform, mhcA, is essential for viability. We have utilized the known physical map position of the gene encoding mhcA to obtain two recessive lethal mutations that virtually eliminate accumulation of mhcA. The mutations are allelic, and the interactions of these alleles with mutations affecting other thick filament components are consistent with the hypothesis that the new mutations lie in the structural gene for mhcA. The homozygous mutant animals move very little and morphological analysis shows that thick filament assembly is severely impaired. Together with the location of mhcA in the center of the thick filament (Miller *et al.*, 1983), the results suggest that mhcA has a unique role in initiating filament assembly. The homozygous mutations have an unexpected effect on morphogenesis that indicates an interaction between the muscle cells and the hypodermis during development. The resultant phenotype may be useful in the search for additional essential muscle genes.

**Key words:** *Caenorhabditis elegans*/filament assembly/myosin/mhcA

## Introduction

Multiple myosin heavy chain isoforms exist in most animals. These isoforms are generally encoded by distinct genes. Even in *Drosophila*, where only a single muscle heavy chain gene is found, multiple isoforms are produced by differential splicing (Rozeck and Davidson, 1986; Bernstein *et al.*, 1986). Typically each isoform is only expressed in a limited subset of the many different muscle types in each animal. The isoforms often have different enzymatic properties *in vitro* and these differences are presumed to account in part for the particular physiological properties of each muscle type. Two or more myosin isoforms are often found within the same muscle cells, although the general significance of this is unknown.

In the nematode *Caenorhabditis elegans* there are a total of four myosin heavy chain muscle isoforms, the products of four genes, all of which have been completely sequenced (Dibb *et al.*, 1989). Two of these isoforms, mhcC and mhcD, are found exclusively in pharyngeal muscles, which act to pump food into the intestine (Epstein *et al.*, 1974; Ardizzi and Epstein, 1987). The other muscle cells of the

animal, including the 95 body wall muscle cells used for locomotion, contain the other two myosin isoforms, mhcA and mhcB (Epstein *et al.*, 1974; Miller *et al.*, 1983), which form predominantly, if not exclusively, homodimers (Schachat *et al.*, 1978). The two isoforms differ in abundance and subcellular location. The mhcB isoform accounts for 75% of the myosin in the body wall cells and is found in the terminal four microns of thick filaments; in contrast mhcA makes up just 25% and lies in the central two microns of the thick filament (Figure 1; Miller *et al.*, 1983). Significantly, this central region includes the so-called 'bare-zone', which marks the reversal of filament polarity (Figure 1). The bare zone also represents the likely site where filament assembly initiates. The differential distribution of the two isoforms within the filament suggests that the two myosin isoforms may have evolved different functional roles in the assembly of the thick filament.

Mutations affecting mhcB have been the subject of several studies. MhcB is the product of the *unc-54* gene (MacLeod *et al.*, 1977) and mutations in the *unc-54* gene are readily isolated (Brenner, 1974; Anderson and Brenner, 1984), including those which completely eliminate mhcB accumulation as well as classes of missense mutations and small in-frame deletions (MacLeod *et al.*, 1977; Moerman *et al.*, 1982). Absence of mhcB results in animals with impaired movement at all stages, but with significant residual movement, especially in early larval stages. Even adults, which are unable to move at all on an agar surface, can thrash weakly in liquid. Thick filaments are reduced in number to ~25% of wild-type, approximately in accord with the decreased amount of total myosin (Epstein *et al.*, 1974). Despite the absence of mhcB in these filaments, they can be as long as wild-type filaments (Mackenzie and Epstein, 1980), indicating that mhcB does not regulate filament length.

In contrast to the hundreds of loss-of-function mutations isolated for the *unc-54* gene (see, e.g. Bejsovec *et al.*, 1984), no mutations eliminating mhcA function have previously been reported. The disparity in the recovery of mutations in the two genes is not due to a difference in target size,

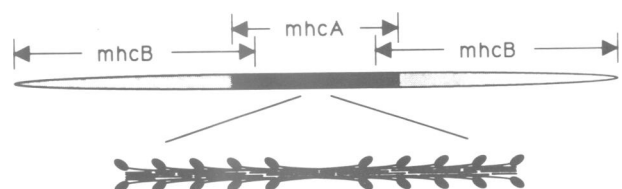


**Fig. 1.** The distribution of the two myosin heavy chain isoforms in the 10  $\mu$ m long nematode thick filament are shown above (Miller *et al.*, 1983). The central ~2  $\mu$ m of the thick filament contains exclusively mhcA and includes the region where the polarity of the filament reverses, as illustrated in the bottom part of the figure, where the myosin molecules are arrayed about rod-like paramyosin molecules and perhaps core proteins (Epstein *et al.*, 1985).

since the two genes are essentially identical in size (Dibb *et al.*, 1989). Instead the absence of *mhcA* null animals in screens used to recover *mhcB* mutations must be accounted for in one of two ways: either animals lacking *mhcA* move almost as well as wild-type, or animals lacking *mhcA* are dead. Either phenotype would be missed in screens for viable animals with altered motility. If the two isoforms were similar in function, then *mhcA* mutations would probably be near wild-type in movement as the more abundant *mhcB* isoform would mask the absence of the *mhcA* isoform. If, however, the *mhcA* protein performs a unique role in either muscle assembly or muscle contraction, as suggested by its exclusive presence in the bare zone, then complete paralysis might result. The recessive lethality of some *unc-54* dominant missense mutations (MacLeod *et al.*, 1977; Dibb *et al.*, 1985; Bejsovec and Anderson, 1988) shows that complete paralysis of the body wall musculature is probably incompatible with viability.

The phenotype of mutants lacking *mhcA* should, accordingly, have important implications for understanding the role of this isoform. When Albertson (1985) localized the *myo-3* gene by *in situ* hybridization to a small region on chromosome 5, and Miller *et al.* (1986) showed that *myo-3* encoded the *mhcA* isoform, it became possible to use marker mutations from the region on chromosome 5 to facilitate screens for mutants lacking *mhcA*. With such a screen one *mhcA*<sup>-</sup> mutant has been recovered and a second allele has been recovered in a more general screen. Loss of *mhcA* leads to a failure of normal thick filament assembly, an inability to move, and developmental arrest in the first larval stage. The failure of effective muscle contraction has an unexpected consequence on morphogenesis, which is described and discussed.

## Results

### Isolation of *myo-3(st378)* and *myo-3(st386)*

The cytogenetic localization of *myo-3* to the right of the actin cluster allowed us to focus on that specific region for mutations which eliminate *mhcA* accumulation. We assumed that loss of *mhcA* would result in lethality, and therefore attempted to recover lethal mutations linked to *sma-1*, a gene lying ~0.5 map units to the right of the actin cluster (Figure 2). Altogether 26 lethal mutations, <5% recombination from *sma-1*, were recovered from 550 F1 clones (see Materials and methods).

We postulated from our previous experience with the recessive lethal alleles of the *unc-54* locus that *mhcA*<sup>-</sup> animals would complete morphogenesis, hatch from the egg but never move. Only one of the 26 linked-lethal mutations, *st378*, fell in this class. Further studies focused on this mutation.

A second mutagenesis was carried out starting with wild-type animals. Among 500 F1 clones examined, a second mutation, *st386*, was recovered which yielded a phenotype similar to the phenotype of the *st378* mutation. The *st386* mutation lies near to *sma-1* and it fails to complement the *st378* mutation.

### Genetic analysis of *st378*

The *st378* mutation has been mapped genetically to a position 0.2% to the right of *sma-1*, and ~0.7% right of the actin cluster (Figure 2; see Materials and methods). This position is consistent with the reported cytogenetic location of *myo-3*.

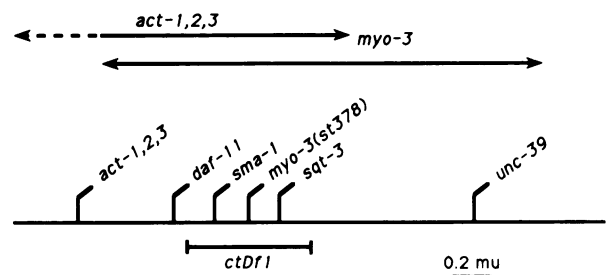


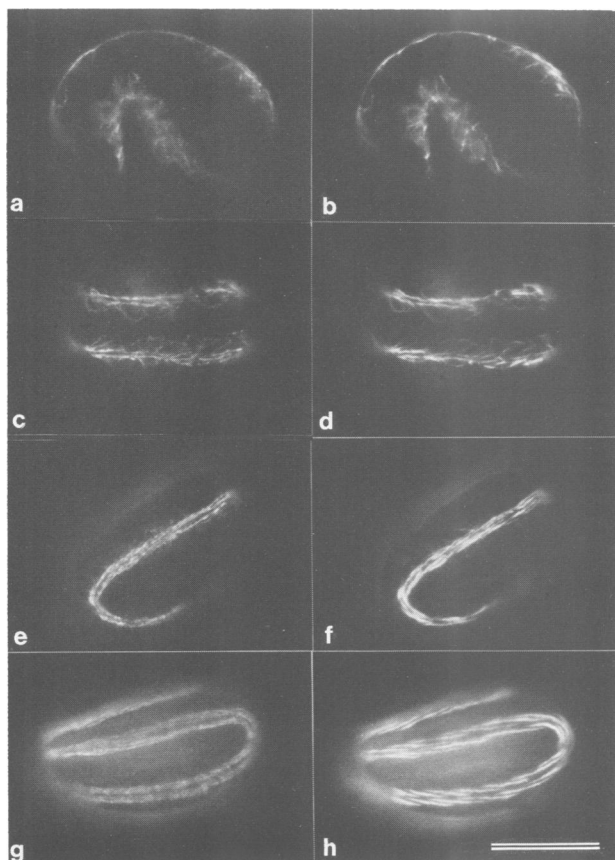
Fig. 2. The relative positions of the actin genes and the *myo3* gene as determined by cytogenetics (Albertson, 1985) are shown above a genetic map of the region of chromosome 5. The position of the *myo3(st378)* mutation is shown relative to other genetic markers used in this study.

Table I. Comparative movements of *myo3* mutants

| Genotype                             | Movement                                      | Viable |
|--------------------------------------|---|--------|
| <i>myo-3(st378)/+</i>                | ~0.8 mm/s                                     | Yes    |
| <i>unc-54(0)/+</i>                   | ~0.8 mm/s                                     | Yes    |
| <i>unc-54(0); sup-3</i>              | ~0.1 mm/s                                     | Yes    |
| <i>unc-54(0); sup-3/+</i>            | ~0.06 mm/s                                    | Yes    |
| <i>unc-54(0)</i>                     | Paralyzed as adult                            | Yes    |
| <i>unc-54(0); sup-3/myo-3(st378)</i> | Paralyzed as adult                            | Yes    |
| <i>unc-54(0); +/-myo-3(st378)</i>    | Paralyzed after hatch; reaches adulthood      | Yes    |
| <i>myo-3(st378)</i>                  | Very slight embryonic movement; arrests as L1 | No     |
| <i>unc-54(0); myo-3(st378)</i>       | Totally paralyzed as embryo                   | No     |

Genetic tests were also carried out to test the hypothesis that *st378* is a loss-of-function allele. The mutation is recessive to the wild-type allele, with heterozygous *st378/+* animals similar to wild-type in their movement and morphology as seen in the dissecting microscope, and in their muscle structure as seen with polarizing light microscopy. The deficiency, *ctDf1*, spans the region from *sma-1* to *sqt-3*, and, when placed in *trans* to the *st378* mutation, fails to complement *st378*; the *st378/ctDf1* animals have a phenotype indistinguishable from *st378/st378* homozygotes. However, the *st378* mutation is not suppressed by the amber suppressor *sup-7* (Waterston, 1981).

In addition to these standard criteria, a loss-of-function allele of the *myo-3* gene would be expected to have predictable effects when placed in combination with mutations of the myosin heavy chain gene *unc-54* and the paramyosin gene *unc-15* (Waterston *et al.*, 1977; Kagawa *et al.*, 1989). A *myo-3* loss-of-function allele should be semi-dominant in an *unc-54(0)* null background, as *unc-54(0)* animals are already compromised in movement and are entirely dependent on *mhcA* for that movement. The *unc-54(0);st378/+* animals were noticeably slower than *unc-54(0);+/+* animals during larval stages (Table I). Although adults of both genotypes failed to move, the *st378* heterozygotes were distinguishable as smaller, sicklier animals. Similarly, since increased amounts of *mhcA* protein are able to rescue partially the uncoordinated phenotype of *unc-15(e73)* heterozygotes (Riddle and Brenner, 1978; Waterston *et al.*, 1982; Miller and Maruyama, 1986), reduced levels of *mhcA* might lead to reduced motility of *unc-15(e73)* animals. Again, *unc-15(e73); st378/+* animals were reliably distinguished



**Fig. 3.** Wild-type embryos of mixed ages were stained with a polyclonal anti-mhc serum (a, c, e and g) and a monoclonal antibody specific for mhcA (b, d, f and h). The embryos are arranged by chronological age from top to bottom. **Panels a and b** are lateral views of a 1½-fold embryo (equivalent to 420 min; Sulston *et al.*, 1983), showing dorsal and ventral quadrants. **Panels c and d** are dorsal views of a slightly older and longer embryo, showing the left and right dorsal quadrants of muscle cells, in which the myosins have already begun to assemble, as evidenced by the striated appearance of the staining. **Panels e and f** are dorso-lateral views of a nearly 2-fold (~450) embryo. Organization is advanced from the earlier embryo. **Panels g and h** show a portion of a fully elongated embryo, in which a single quadrant is in focus in each of the three segments of the embryo. Striations are well formed and represent the assemblages of the myosin-containing thick filaments into A-bands (see Figure 6). Bar = 20 µm.

from their *unc-15(e73)* siblings by their more severe paralysis.

Another test of the nature of the *st378* mutation is provided by *sup-3* mutations, which result in increased accumulation of mhcA (Riddle and Brenner, 1978; Waterston *et al.*, 1982) as a result, in at least some cases such as *e1407*, of tandem duplications which include the *myo-3* gene (Miller and Maruyama, 1986). These suppressors act on *unc-54* loss-of-function mutants and the missense mutation *unc-15(e73)* to improve motility. The movement of *unc-54* animals is directly correlated with increased copy number of the *myo-3* locus (R.H. Waterston, unpublished; Miller and Maruyama, 1986). Thus *unc-54(0);sup-3/sup-3* animals move better than *unc-54(0);sup-3/+* animals and these in turn move better than *unc-54(0);+/+* animals (Table I). By extension, an *unc-54(0);sup-3/+* animal should move better than an *unc-54(0);sup-3/myo-3<sup>-</sup>* animal. Further, the *unc-54;sup-3/myo-3<sup>-</sup>* animal should resemble an *unc-54(0);+/+* animal and be better moving than an *unc-54(0);+/myo-3<sup>-</sup>* animal. These predictions were borne out (Table I). These con-

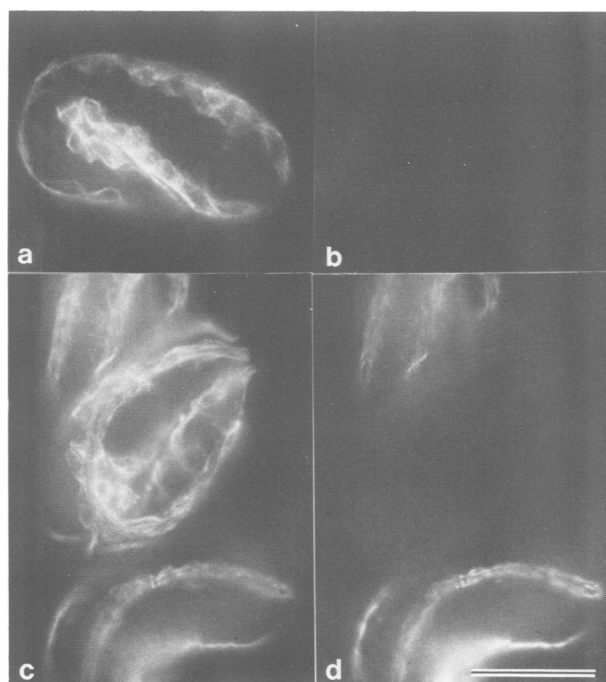


**Fig. 4.** The *myo-3(st386)* embryos have been stained as in Figure 3: on the left are embryos stained with the anti-myosin polyclonal and on the right are embryos stained with the mhcA monoclonal. **Panels a and b** depict a 1½-fold embryo similar in age to those shown in Figure 3a–d. A strong signal was obtained with the anti-myosin antibody, but no signal above background was apparent with the anti-mhcA monoclonal antibody. **Panels c and d** show a typical older mutant animal in the center of the field along with heterozygous animals above and below. Only a very faint staining with the monoclonal antibody can be detected in the *st386* embryo. The mhcB is poorly organized and some remains in the cell body as shown by its outlining of muscle nuclei. (Compare with Figure 3e–h.) The muscle cells from the dorsal quadrant lie against the cuticle anteriorly and posteriorly, but fail to follow the outside of the animal in the curved central portion. Instead they cross to the ventral surface. The *st378* embryos give similar images. Bar = 20 µm.

structions also yielded the presumed *unc-54(0);myo-3<sup>-</sup>* double mutant, which was inviable and showed no visible movement of the body wall muscles (see below).

#### **Effects of the *st378* and *st386* mutations on muscle function and development**

In order to assess the effect of *st378* and *st386* on embryonic development and movement, eggs from heterozygous parents were followed throughout development. For *st378*, the linked *sma-1* mutation, which itself affects morphogenesis, was first removed by recombination. The *st378* embryos could not be distinguished from their siblings until elongation began. The *st378* embryos elongated more slowly than wild-type, and never progressed beyond a 2-fold extension, whereas wild-type reached >3-fold, before ceasing elongation. In addition, the twitching of the body wall muscles that is prominent as wild-type begins to elongate was significantly reduced in the *st378* embryos, and the later movements of the entire embryo were completely lacking in *st378* animals. Instead, movements were limited to slight displacements of the tips of the head and tail regions. Despite the failure to elongate, other developmental events continued to occur, such as pharyngeal morphogenesis and cuticle deposition. Pharyngeal pumping began slightly later than in wild-type and hatching was generally delayed by 90 min or more. Pumping continued sporadically after hatching and bacterial

ghosts were apparent in a dilated anterior gut lumen. Even after hatching the animals remained in a folded state and never showed any sign of locomotion. The animals persisted in this arrested state for days and eventually died without significant growth. Similar observations were made for the *st386* embryos. The *unc-54: sma-1 st378* mutant animals also arrested elongation at a 2-fold stage, yet hatched. They showed no movements of the body wall muscles, not even twitching of the tips of their heads or tails. Their pharynges pumped, similar to *st378* animals.

#### Effects of the *st378* and *st386* mutations on muscle organization

Developing embryos were fixed and stained with antibodies directed against the two body wall muscle isoforms. In wild-type, *mhcA* and *mhcB* are diffusely distributed in early muscle cells, but between the 1½-fold and 2-fold stages, the myosins become localized near the sarcolemma adjacent to the hypodermis, where they are organized into nascent sarcomeres (Figure 3a–d). In later stages the sarcomere structure is more apparent and myosins are limited to the sarcomere (Figure 3e–h). The *st378* and *st386* embryos fail to accumulate significant levels of anti-*mhcA* reactive material, although in late embryos a slight signal is detectable with the antibodies used (Figure 4b and d). The anti-*mhcB* reactive material remains dispersed in the muscle cells in early embryos (Figure 4a) but in later embryos much of the myosin is in poorly organized aggregates (Figure 4c). Even in these embryos, however, some myosin remains dispersed, often outlining the muscle cell nuclei. Actin in *st378* embryos, as revealed by the mushroom toxin phalloidin, is localized near the sarcolemma, but fails to assume the wild-type striated distribution (data not shown).

The locations of some muscle cells are also abnormal in the *st378* and *st386* embryos. Muscle cells follow the inner (ventral) and outer (dorsal) curves of the wild-type *C. elegans* embryo. In the older mutant muscles, the muscle cells are absent along part of the outer curve and are displaced ventrally, forming a more or less straight strip of cells stretching from an anterior dorsal position across the inner curve of the fold to a posterior dorsal position (Figure 4c). Cells further anterior or posterior on the dorsal surface are not commonly displaced, nor are the ventral cells. The precise area involved along the outer curve varied from animal to animal, and even quadrant to quadrant, but displaced muscles were found in every older homozygous mutant embryo examined.

In electron micrographs of the arrested *st378* embryos abnormalities of both the filament lattice and the hypodermal cell–muscle cell boundary were apparent. In wild-type, myofilaments are restricted to the sheet of muscle cytoplasm adjacent to the hypodermis. The myosin-containing thick filaments and the actin-containing thin filaments lie in an ordered lattice (Figure 5). In the mutant the myofilaments remain near the hypodermal surface, but the clusters of myosin-containing thick filaments, which normally make up the A-bands characteristic of wild-type muscle, are absent (Figure 6a). Instead large filaments of variable diameter are found sparsely scattered in the lattice (Figure 6b). These filaments are generally longitudinally oriented as in wild-type, but many are irregular in outline or larger in diameter than normal thick filaments. They resemble the paracrystalline arrays of paramyosin found in mutants with

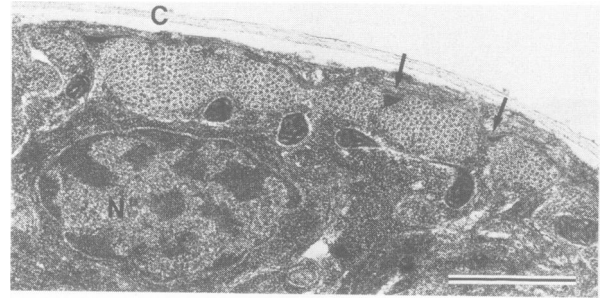


Fig. 5. The muscle organization of a wild-type first-stage larva (0–4 h after hatching) is shown as visualized with transmission electron microscopy. The myofilament lattice is near the top of the figure, lying just under the extracellular cuticle (C) and very thin hypodermis. The longitudinally oriented filaments are cut in cross-section in this transverse section. The larger diameter thick filaments are grouped together into A-bands, which are separated from one another by regions that contain only thin filaments (the I-bands). The boundaries of one such unit are indicated by a pair of arrows, the left of which also points to a triangular shaped dense-body (equivalent of the vertebrate Z-line) in the middle of an I-band. The body of the muscle cell with a prominent nucleus (N) lies in the bottom portion of the figure. Bar = 1  $\mu$ m.

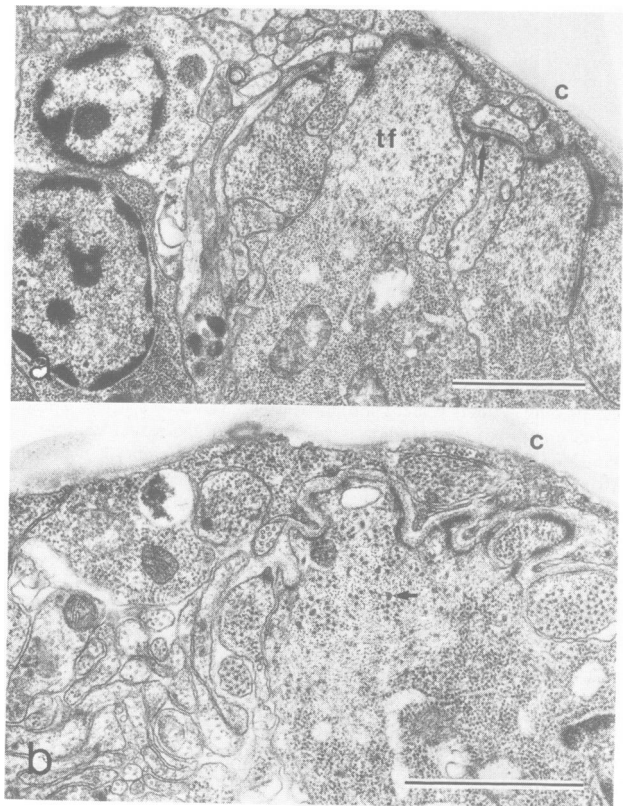
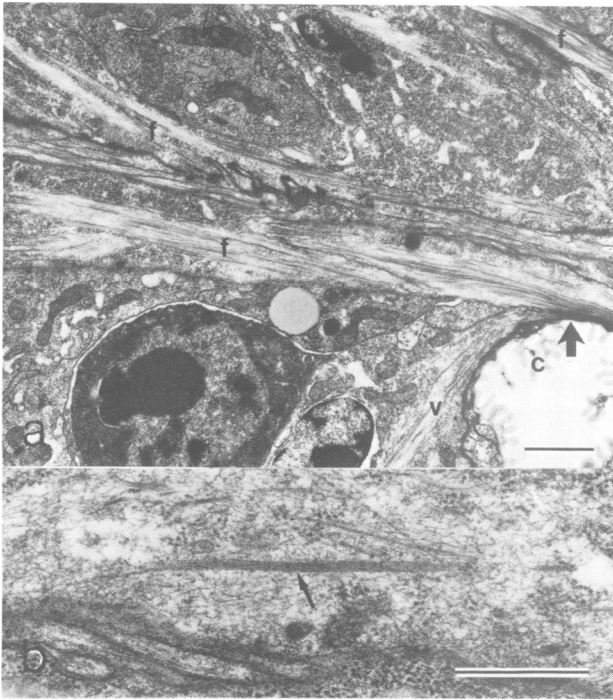
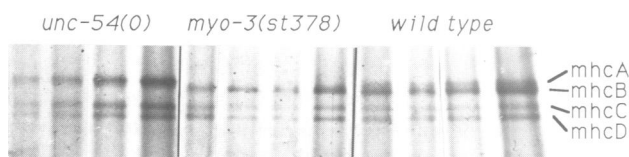


Fig. 6. The muscle organization of two *sma-1 st378* first-stage larvae is shown as visualized with transmission electron microscopy (see Waterston, 1988 for review of muscle structure). In both panels the animals are oriented similarly to the wild-type embryo in Figure 5, with the cuticle (C) near the top of each field and portions of several muscle cells in the right two-thirds of each panel. Boundaries of the cells are distorted compared to wild-type, but the filaments are still oriented longitudinally. They lie in the region of the cell adjacent to the hypodermis, as they would in wild-type. Thin filaments (tf) are prominent but thick filaments are relatively scarce. The larger diameter filaments are often of irregular size and shape (panel b, arrow). Densities along the muscle cell membrane presumably represent incompletely formed dense bodies. Bars = 1  $\mu$ m.



**Fig. 7.** Approximately sagittal sections of *unc-54;myo-3(st378)* larvae show, in **panel a**, a portion of a muscle cell coursing from the dorsal quadrant to the ventral and in **panel b**, a large diameter filament. The plane of section is similar to the optical plane of section of the embryo in Figure 4c, but the embryo is oriented so that the inner curve of the folded larva is present at the lower right (arrow) and the outer curve is above the field. Longitudinally sectioned thin filaments (f) are apparent and indicate the orientation of the muscle cells themselves. Filaments and cells pass from the right to the left in field, or from dorsal to ventral in the embryo. One of the cells coming from the dorsal surface appears to replace the ventral cell (v) along the hypodermal surface (arrow). Folded and branched cuticular structures (c) present along the inner curvature may be secondary to the failure to elongate. At higher magnification in panel b a large diameter filament (arrow) has a striated appearance, not dissimilar to paramyosin paracrystals seen in paramyosin-affecting mutants. (a) Bar = 2  $\mu\text{m}$ ; (b) Bar = 0.5  $\mu\text{m}$ .



**Fig. 8.** Myosin heavy chains from different loadings of mutant and wild-type first-stage larvae are compared on SDS gel electrophoresis. In the center four lanes, myosins from the *st378* animals are shown, with wild-type on the right and *unc-54(0)* on the left. The four myosin heavy chains differ slightly in mobility as indicated at the right. In the *st378* lane mhcA is lacking and in the four *unc-54* lanes mhcB is absent. The amount of mhcA in the *unc-54* lanes is proportionately higher than in wild-type as these animals also contained *sup-3* to facilitate collection of sufficient first-stage larvae.

altered paramyosin *unc-15* and *unc-82* (G.R.Francis and R.H.Waterston, unpublished; Waterston *et al.*, 1977, 1980; Kagawa *et al.*, 1989; L.A.Schriefer and R.H.Waterston, unpublished). These arrays are particularly apparent in the *unc-54;myo-3* double mutants: in longitudinal sections periodic repeats in the staining intensity are visible, similar to those seen in *unc-82* paracrystals (Figure 7b). Longitudinal sections also demonstrate the ventral displacement of dorsal muscle cells (Figure 7a).

Other muscle structures are also affected. Dense bodies, the nematode equivalent of the Z-lines of cross striated muscle, are incompletely formed in the *myo-3* mutants: their bases along the sarcolemma are obvious, but the structures fail to extend into the cell to divide the lattice into sarcomeres (Figure 6). Thin filaments are numerous and generally longitudinally oriented, apparently attached to the stunted dense bodies. The cell margin adjacent to the hypodermal cell is often not smooth as in wild-type but instead has a deeply folded appearance.

#### Protein analysis of *st378* animals

The *mhcA* isoform can be distinguished from the other myosins by monoclonal antibodies specific for each isoform and also by its distinctive mobility on SDS gels (Miller *et al.*, 1983; Otsuka, 1985). The immunofluorescent staining of the arrested *st378* larvae, described above, showed that they contained little, if any, *mhcA*. To obtain a measure of the amounts of *mhcA*, independent of the antibody reactivity of the molecules, a method was developed to separate the arrested *st378* L1 larvae from their viable siblings in sufficient quantities to permit direct detection of myosin in SDS-acrylamide gels. The results show *mhcA* is significantly reduced, if not absent, in *st378* animals, but other myosins are unaltered (Figure 8). The pattern of protein bands other than myosin is also similar between *st378* and wild-type animals (data not shown). Nor was an *mhcA* protein of altered mobility detected in similar preparations transferred to nitrocellulose membranes and analyzed using the *mhcA*-specific monoclonal antibodies.

#### Discussion

The successful effort to acquire mutations in the *myo-3* gene by taking advantage of the known map location of the gene has produced evidence that the *mhcA* protein plays a unique role in thick filament assembly. The unexpected effects of the *myo-3* mutations on development suggest that an interaction occurs between the developing muscle and hypodermal cells. The failure of previous screens for muscle mutants to uncover defective alleles of this gene indicate that other muscle genes of this class could be discovered by employing screens for mutants with similar phenotypes. Finally the combination of physical mapping and classical genetics applied here should be applicable to other instances where *in vivo* function of a protein needs to be determined.

Three lines of evidence presented here support the contention that *st378* and *st386* are mutations in the *myo-3* locus. They are in the region predicted from the cytogenetic analysis. The mutations affect primarily body wall muscle, both functionally and structurally, indicating that the gene encodes a component of muscle. The muscle component most drastically altered is *mhcA* which is barely detectable with a *mhcA*-specific antibody and significantly reduced in SDS gels of total mutant proteins. These arguments are, none the less, indirect and other explanations of the data are tenable. However, the data were highly suggestive and led us to attempt the experiments described in the accompanying paper (Fire and Waterston, 1989). The complementation of both mutations via a transfected *myo-3* gene leaves little doubt that the mutations are in the *myo-3* gene.

The *st378* and *st386* mutations are probably loss-of-function mutations. The most direct evidence comes from

examining the levels of *mhcA* in *st378* animals with either the antibodies or SDS gels; these make it clear that little intact *mhcA* accumulates. Other evidence that *st378* is a loss-of-function allele comes from the genetic experiments. The mutations are recessive in a wild-type background. The *st378* homozygotes are similar to *ctDf1/st378* animals. The dose-dependent phenotypes associated with *st378* in *unc-54* and *unc-15* backgrounds are consistent with expectations for a *myo-3* null and the interactions of the *st378* in *trans* to the *sup-3* mutations in the various genetic backgrounds show that these dominant effects can be eliminated simply by supplying additional *mhcA* product. The similarity of the *st386* allele to *st378* in various tests argues that it too is a loss-of-function allele. The mutation frequency of  $>10^{-3}$  per mutagenized gamete for the gene, although based on small numbers, is also similar to the forward mutation frequency of the *unc-54* gene in *C.elegans* of  $1.6 \times 10^{-3}$  (S.Brenner, unpublished; Anderson and Brenner, 1984).

The arguments that *st378* and *st386* are loss-of-function alleles are thus indirect. A class of missense mutations in the *unc-54* gene has been described with some features similar to the *myo-3* mutations, in that they are recovered at high frequency, and lead to loss of accumulated product (*mhcB*). They differ from the *myo-3* mutations in that they are all semi-dominant. The *st378* and *st386* mutations show no evidence of antimorphic activities and in the accompanying paper (Fire and Waterston, 1989), it is shown that even two copies of the *st378* allele are recessive to a single *myo-3* transgene.

The paucity of movements in *st378* animals indicates that the more abundant *mhcB* substitutes very poorly for *mhcA*. The *mhcA* isoform must then have a unique role in assembly and/or contraction of body wall muscles. Several unique roles for *mhcA* can be imagined. Deposition of *mhcA* on the nascent filament may necessarily precede the addition of *mhcB*. Another possibility is that *mhcB* and paramyosin may assemble in the absence of *mhcA* but only into unipolar filaments, which would be incapable of generating force. A third alternative is that the absence of *mhcA* from thick filament assemblages might result in a failure to localize the filaments properly. Other possibilities including temporal differences in the appearance of the two isoforms in development might also be considered. The morphological analysis presented here favors the idea that *mhcA* assembly obligatorily precedes *mhcB* assembly. Consistent with this, immunofluorescent images indicate that some *mhcB* remains dispersed in the cells rather than localizing to the myofibril lattice. The reduced abundance of thick filaments in electron micrographs also indicates a failure of *mhcB* assembly. The often irregular size and outline of the residual large filaments in *st378* animals may represent paramyosin with possible core structures (Epstein *et al.*, 1985).

The additional effects of the *st378* mutation on elongation, muscle cell placement and viability are unlikely to be due to adventitious, closely linked mutations. No separation of the various aspects of the *st378* phenotype has been observed in the mapping studies and the *st386* isolate and the *st378/st386* double heterozygote also result in the same phenotypic changes as *st378*. Muscle cell displacement and lethality have been noted with severe alleles of *unc-54* and *unc-15*, but elongation is normal in these mutants.

Priess and Hirsh (1986) have hypothesized that elongation in wild-type occurs through a compressive circumferential

force exerted in the hypodermis. The failure to elongate then implies that there is a defect in the hypodermis in addition to the observed body wall muscle defect. If *mhcA* had a role in cytoplasmic motility, its absence in the hypodermis might lead to a failure of the embryo to elongate. Alternatively, the body wall muscle cells and the adjacent hypodermis may interact during development and a defect in one might lead to a secondary defect in the other. We favor the second explanation for several reasons. Cytoplasmic myosins in other organisms are the product of distinct genes and have quite different sequence features from striated muscle myosins (Warrick and Spudich, 1987); the *mhcA* sequence clearly places it among the striated muscle myosins (Dibb *et al.*, 1989). Further, other cell movements appear normal and elongation does proceed part way. Evidence for hypodermal-muscle cell interaction already exists in that intermediate filaments and associated structures become specifically localized above the muscle cells as the embryo begins to elongate (G.R.Francis and R.H.Waterston, unpublished). The nature of the signals between the tissues and how the failure of muscle to contract disrupts such signals is unclear. Nor is it obvious why the muscle cells become displaced. Yet recent observations with additional muscle mutants show that the failure to elongate is a common feature and that often muscle displacement occurs in these mutants as well (L.Venolia, unpublished; B.D.Williams, unpublished; R.J.Barstead, unpublished).

The reason for the arrest of the animals is unclear. The embryos hatch and the larvae do feed. This food may, however, not pass down the intestine as evidenced by the dilated anterior intestinal lumen. The displaced muscle cells may compress the intestine to block passage or defecation may be impaired, as *mhcA* is also present in intestinal and anal muscles (Ardizzi and Epstein, 1987). Starved first-stage wild-type larvae can persist for several days before death and the *st378* larvae may be in a similar state before eventually succumbing to lack of nutrition.

This work has two more general implications. It demonstrates the feasibility in *C.elegans* of moving from a known protein to the recovery of mutations in the gene for that protein, using a combination of physical mapping and genetics. In this case we took advantage of the cytogenetic determination of the position of the gene, but the construction of a physical genomic map consisting of a series of overlapping cloned fragments should permit the rapid mapping of any cloned sequence (Coulson *et al.*, 1986, 1988). The relatively high mutation frequency in *C.elegans* after ethylmethanesulfonate (EMS) mutagenesis (Brenner, 1974) makes it feasible to recover mutations in any gene, even in cases where no visible phenotype is associated with alterations in a gene product (Sulston *et al.*, 1975; McGhee and Cottrell, 1986). The approaches used here, although certainly more arduous than gene replacement in yeast, offer a feasible means to carry out reverse genetics until appropriate methods are developed to achieve gene transplacement in *C.elegans*.

Secondly, this work demonstrates that there is a class of undiscovered muscle genes in *C.elegans*, where loss-of-function alleles lead to lethality. Lethal alleles of the *unc-45* gene have also recently been recovered and available evidence favors the interpretation that these are loss-of-function alleles (L.Venolia and R.H.Waterston, in preparation). In the course of isolating the *st386* mutation,

a second mutation, *st385*, was isolated which appears to identify a new essential muscle gene on linkage group 4 (R.J. Barstead and R.H. Waterston, unpublished). Larger scale screenings are in progress to identify further mutations in genes whose products are essential for muscle function and development (B.D. Williams and R.H. Waterston, unpublished).

## Materials and methods

### Genetic methods and strains

General methods for culturing, handling and EMS mutagenesis of *C. elegans* have been described by Brenner (1974) and in Wood *et al.* (1988). The N2 wild-type strain of *C. elegans* var Bristol was the parent of all strains used in this work. All experiments were performed at 20°C unless stated otherwise.

The genes and mutations used in this study were as follows. LGI: *dpy-5(e61)*, *unc-15(e73)*, *unc-54(e1315)*, *unc-54(e190)*; LGII: *bli-2(e768)*; LGIII: *unc-32(e189)*; LGIV: *dpy-13(e184)*, *unc-22(e66)*, *dpy-20(e2017)*; LGV: *dpy-11(e224)*, *unc-42(e270)*, *daf-11(m47)*, *sma-1(e30)*, *sqt-3(e24)*, *sup-3(e1407)*, *unc-39(e257)*; LGX: *sup-7(st5)* (Waterston, 1981), *lon-2(e678)*. In addition three chromosome rearrangements were used: the reciprocal translocation *DnT1 (IV;V)*, which carries a dominant Unc mutation, *unc-(n754)*, and a recessive lethal mutation acts as an effective balancer for chromosomes IV R and V (Ferguson and Horvitz, 1985); *ctDf1*, a small deficiency extending from *sma-1* to *sqt-3* (Wood and Kramer, personal communication); and *eDf1*, a complex rearrangement which contains an amplification of the *myo-3* locus and suppresses recombination in the *unc-42:myo-3* interval. Strains were obtained either from the Cambridge collection or the Caenorhabditis Genetics Center unless otherwise noted.

### Generation of *st378*

*sma-1(e30)* hermaphrodites were treated with 0.025 M EMS for 4 h and were mated after overnight recovery with *daf-11(m47)* males. Single cross progeny were placed onto separate plates at 25°C and allowed to reproduce. Animals which yielded only rare, fertile Sma animals were assumed to have a lethal mutation linked to *sma-1*, and phenotypically wild-type animals were picked to propagate the strain. Synchronized broods were used to determine the stage of arrest associated with the induced mutation. Those which arrested between late embryogenesis and the late first larval stage were examined for altered movement.

The *st378* mutation was recombined away from the *sma-1* marker by mating *sma-1 st378 +/+ + unc-39* males with *sma-1 unc-39* hermaphrodites, and selecting wild-type recombinant progeny. One of six such progeny proved to be *+ st378 +/sma-1 + unc-39*. Also during propagation of the *sma-1 st378 +/+ + unc-39* strain, a *st378 +/+ unc-39* animal was fortuitously picked. The mutant phenotypes produced from the two different *st378* recombinants were identical.

### Mapping of *st378* and *st386*

To determine the position of *st378* relative to *sma-1*, five Sma recombinant animals were recovered among 2988 viable progeny of *+ sma-1 st378/unc-42 + +* parents. None of the Sma recombinants included the *unc-42* marker mutation, thus placing the *st378* mutation 0.25 map units to the right of *sma-1*. From *sma-1 st378 +/+ + sqt-3* parents four viable Sma recombinant progeny each contained *sqt-3*. From *sma-1 st378 +/+ + unc-39* parents three viable Sma recombinant progeny each contained *unc-39*. The *sma-1 (4/19) sqt-3 (15/19) unc-39* order was determined separately. A two factor estimate of the linkage of *st378* and *sqt-3* was made from finding 2 + + chromosomes among 1374 wild-type progeny of *sma-1 st378 +/+ + sqt-3* parents, giving a value of 0.14 m.u. (Figure 2).

### Genetic interactions

To evaluate the *st378* mutation in *unc-54* and *unc-15* backgrounds, progeny of *unc-54(e190)/+;sma-1 st378/+ +* or *unc-15(e73)/+;sma-1 st378/+ +* animals were compared with segregants from *unc-54/+ or unc-15/+* parents, and scored as either wild-type, Unc, severe Unc or lethal. The severe Uncs were distinguished from Uncs based on their complete failure by the fourth larval stage to move along the agar surface, and by their sickly appearance and virtual absence of fertilized eggs in the adult stage. If *unc-54;st378/+* and *unc-15;st378/+* animals are severe Uncs, the expected proportions would be 9:1:2:4 for wild:Unc:SevUnc:Let. For *unc-54* the observed proportions were 140:16:22:52 (predicted 129:14:29:58) and for *unc-15* the proportions were 101:8:22:42 (predicted 97:11:22:43). Severe

Uncs were seen only infrequently in the control broods from *unc-54/+ or unc-15/+* parents.

To evaluate the effects of *sup-3* mutations in *trans* to *st378*, *unc-54(e1315)/+; sup-3(e1407)/sma-1 st378* F1 animals were generated. Both suppressed Uncs and Uncs were present among their progeny and it was possible to propagate lines of *unc-54;sup-3/sma-1 st378* animals simply by selecting the Unc animals and these animals were used to generate the *unc-54; sma-1 st378* animals.

The *st378* mutation was tested for suppression by the amber suppressor *sup-7(st5)*. Animals of the *dpy-20;sma-1 st378/+ +;sup-7/+* genotype were constructed and their progeny were inspected for any Sma animals with improved movement. No evidence of suppression was observed.

### Biochemical methods

SDS-polyacrylamide gels were run as described (Otsuka, 1985) using a 3% polyacrylamide separating gel, bonded to one plate with dimethyl, dichlorosilane (Garoff and Ansoorge, 1981). Twenty cm gels were run at 35 mA constant current until the dye front reached the bottom. Samples were prepared by boiling whole worms in SDS sample buffer. Gels were silver stained as described (Merrill *et al.*, 1981).

L1 larvae of the stated genotypes were prepared in the absence of *Escherichia coli* by hatching eggs prepared by the hypochlorite-alkali method in M9 (Wood *et al.*, 1988). The suspension of mixed animals and unhatched eggs was placed in a Petri dish and gently swirled. Unhatched eggs were simply removed by aspiration, taking advantage of their tendency to aggregate. The *st378* larvae could be separated from their siblings because the longer, thinner siblings collected more rapidly in the center of the dish and were removed by aspiration. The *st378* larvae moved to the center more slowly and were collected separately. Two or three cycles of the procedure were generally sufficient to produce populations comprised of >95% *st378* animals, with the major contamination consisting of unhatched eggs. As many as 40 000 animals were collected in this manner.

### Microscopy

Animals were observed by Nomarski optics as described in Wood *et al.* (1988). Immunofluorescence was performed on hypochlorite treated eggs, prepared as described (Francis and Waterston, 1985). Monoclonal antibodies were the gift of D. Miller and H. Epstein. Animals were prepared for electron microscopy as follows. Eggs from animals of the appropriate genotype were recovered from adults and allowed to hatch overnight in the absence of food. Animals with the *st378* phenotype were fixed in glutaraldehyde for 1 h, then cut in half and fixed overnight. The remainder of the procedure followed published procedures (Wood *et al.*, 1988).

## Acknowledgements

I thank Kathy Kellerman for help in the initial mutant hunt, J. Nichol Thomson for help with the electron microscopy, Jonathan Hodgkin for suggestions on the genetic analysis and Andy Fire for encouragement and comments on the manuscript. I also thank Sydney Brenner and John Sulston for allowing me to work at the MRC Laboratory of Molecular Biology during my sabbatical. This work was supported in part by the John Simon Guggenheim Foundation and by USPHS grant GM23883. Some strains were obtained from the Caenorhabditis Genetics Center, which is supported by Contract N01 RR-4-2111 between the NIH Division of Research Resources and Curators of the University of Missouri.

## References

- Albertson, D. (1985) *EMBO J.*, **4**, 2493–2498.
- Anderson, R.P. and Brenner, S. (1984) *Proc. Natl. Acad. Sci. USA*, **81**, 4470–4474.
- Ardizzi, J.P. and Epstein, H.F. (1987) *J. Cell Biol.*, **105**, 2763–2770.
- Bejsovec, A. and Anderson, P. (1988) *Genes Dev.*, **2**, 1307–1317.
- Bejsovec, A., Eide, D. and Anderson, P. (1984) In Borisy, G. *et al.* (eds), *Molecular Biology of the Cytoskeleton*. Cold Spring Harbor Laboratory Press, Cold Spring Harbor, NY, pp. 267–270.
- Bernstein, S.I., Hansen, C.J., Becker, K.D., Wassenberg, D.R., Roche, E.S., Donady, J.J. and Emerson, C.P. (1986) *Mol. Cell. Biol.*, **6**, 2511–2519.
- Brenner, S. (1974) *Genetics*, **77**, 71–94.
- Coulson, A.R., Sulston, J., Brenner, S. and Karn, J. (1986) *Proc. Natl. Acad. Sci. USA*, **83**, 7821–7825.
- Coulson, A.R., Waterston, R.H., Kiff, J., Sulston, J. and Kohara, Y. (1988) *Nature*, **335**, 184–186.
- Dibb, N.J., Brown, D.M., Karn, J., Moerman, D.G., Bolten, S.L. and Waterston, R.H. (1985) *J. Mol. Biol.*, **183**, 543–551.

- Dibb,N.J., Maruyama,I.N., Krause,M. and Karn,J. (1989) *J. Mol. Biol.*, **205**, 203–213.
- Epstein,H.E., Waterston,R.H. and Brenner,S. (1974) *J. Mol. Biol.*, **90**, 291–300.
- Epstein,H.E., Miller,D.M., III, Ortiz,I. and Berliner,G.C. (1985) *J. Cell Biol.*, **100**, 904–915.
- Ferguson,E.I. and Horvitz,H.R. (1985) *Genetics*, **110**, 17–72.
- Fire,A. and Waterston,R.H. (1989) *EMBO J.*, **8**, 3419–3428.
- Francis,G.R. and Waterston,R.H. (1985) *J. Cell Biol.*, **101**, 1532–1549.
- Garoff,H. and Ansorge,W. (1981) *Anal. Biochem.*, **115**, 450–457.
- Kagawa,H., Gengyo,K., McLachlan,A.D., Brenner,S. and Karn,J. (1989) *J. Mol. Biol.*, **207**, 311–333.
- Mackenzie,J.M., Jr and Epstein,H.E. (1980) *Cell*, **22**, 747–755.
- MacLeod,A.R., Waterston,R.H., Fishpool,R.M. and Brenner,S. (1977) *J. Mol. Biol.*, **114**, 133–140.
- McGhee,J.D. and Cottrell,D.A. (1986) *Mol. Gen. Genet.*, **202**, 30–34.
- Merril,C.R., Goldman,D., Sedamn,S.A. and Ebert,M.H. (1981) *Science*, **211**, 1437–1438.
- Miller,D.M. and Maruyama,I. (1986) *UCLA Symp. Mol. Cell. Biol. New Ser.*, **29**, 629–638.
- Miller,D.M., Ortiz,I., Berliner,G.C. and Epstein,H.E. (1983) *Cell*, **34**, 477–490.
- Miller,D.M., Stockdale,F.E. and Karn,J. (1986) *Proc. Natl. Acad. Sci. USA*, **83**, 2305–2309.
- Moerman,D.G., Plurad,S., Waterston,R.H. and Baillie,D.L. (1982) *Cell*, **29**, 773–781.
- Otsuka,A. (1985) *UCLA Symp. Mol. Cell. Biol. New Ser.*, **29**, 619–628.
- Priess,J.R. and Hirsh,D.I. (1986) *Dev. Biol.*, **117**, 156–173.
- Riddle,D.L. and Brenner,S. (1978) *Genetics*, **89**, 299–314.
- Rozek,C.E. and Davidson,N. (1986) *Cell*, **32**, 23–34.
- Schachat,F.H., Harris,H.E. and Epstein,H.F. (1978) *Cell*, **15**, 405–411.
- Sulston,J., Dew,M. and Brenner,J. (1975) *J. Comp. Neurol.*, **163**, 215–226.
- Sulston,J.E., Schierenberg,E., White,J.G. and Thomson,J.N. (1983) *Dev. Biol.*, **100**, 64–119.
- Warrick,H.M. and Spudich,J.A. (1987) *Annu. Rev. Cell Biol.*, **3**, 379–421.
- Waterston,R.H. (1981) *Genetics*, **97**, 307–325.
- Waterston,R.H. (1988) In Wood,W.B. *et al.* (eds), *The Nematode Caenorhabditis elegans*. Cold Spring Harbor Laboratory Press, Cold Spring Harbor,NY, pp. 281–335.
- Waterston,R.H., Fishpool,R.M. and Brenner,S. (1977) *J. Mol. Biol.*, **117**, 679–697.
- Waterston,R.H., Thomson,J.N. and Brenner,S. (1980) *Dev. Biol.*, **77**, 271–302.
- Waterston,R.H., Moerman,D.G., Baillie,D. and Lane,T.R. (1982) In Schotland,D.L. (ed.), *Disorders of the Motor Unit*. Wiley and Sons, pp. 747–760.
- Wood,W.B. *et al.* (1988) *The Nematode Caenorhabditis elegans*. Cold Spring Harbor Laboratory Press, Cold Spring Harbor, NY.

Received on June 8, 1989